International Journal of Heat and Mass Transfer 52 (2009) 3197–3204

Contents lists available at ScienceDirect

International Journal of Heat and Mass Transfer

journal homepage: www.elsevier.com/locate/ijhmt

Contact angle and rivulet width hysteresis on metallic surfaces. Part II: With cooled surface

Andrzej Gajewski *

Bialystok Technical University, Faculty of Civil Engineering and Environmental Engineering, Department of Heat Engineering, Wiejska 45E, 15-351 Bialystok, Poland

ARTICLE INFO

Article history:
Received 23 December 2008
Accepted 12 February 2009
Available online 26 March 2009

Keywords:
Contact angle
Rivulet
Hysteresis
Liquid–gas interfaces
Solid–liquid interfaces
Laser methods

ABSTRACT

The results of contact angle and width of the rivulets measurements on plain surfaces made of aluminium, brass and copper are presented in the paper. The measurements were done for the rise, decreasing and again increasing of flow rate on the cooled plates. As a result the hysteresis of contact angle and rivulet width was revealed. It was also noticed that aluminium and brass at certain flow conditions can lose their hydrophobic properties and became the hydrophilic materials. The worst wetting properties were observed for copper. It is supposed that the more electrons on the last shell are the more hydrophilic metal is under flow conditions. Lower temperature improves the wetting properties of the metals and favours the disappearance of the oxide barriers on aluminium and zinc (brass is an alloy of zinc and copper). Since the contact angles on two rivulet edges differ, it is not justified to assume a segment of a circle as the rivulet cross section shape.

1. Introduction

Many processes occurring in cooling towers, surface condensers and environmental engineering or protection use thin liquid layers in forms of the rivulets to heat or mass transfer.

Experimental investigations of the rivulets by Towell and Rothfeld [2] as well as Semiczek-Szulc and Mikielewicz [3] were carried out without at negligible temperature difference among the wall surface, the rivulet and surrounding air. At the investigations by Hirasawa and Hauptmann [4] as well as at those presented in the part I [9] the wall surface temperature was higher than the surrounding air temperature as well as the rivulet temperature. These conditions did not promote existence of the liquid microfilm on the surface in the close neighbourhood of the rivulet. The similar situation took place in the experiments of Sutjiadi-Sia and Eggers [7], where high pressure prevented the liquid from evaporating and the liquid microfilm on the solid phase can not come to existence.

In order to investigate the temperature impact on the wetting properties the experiments described in the paper were carried out keeping temperature of the plate surface lower than the temperature of surrounding air as well as the rivulet. However this temperature was maintained higher than dew-point temperature, so that there was no condensation condition.

Comparisons of the water rivulet wetting properties and the differences in the rivulets' behaviour on the heated and cooled surfaces are the main goals of this research.

2. Experiment

The approach by Langmuir and Schaefer [1], developed and applied also by the author, was used in the present study as the measurement method. The investigation method and the measurement uncertainties analysis are described in details in work [8]. The experimental set-up and the measuring procedure are presented in the part I [9]. The temperature of the plates was kept about 5÷8 °C lower than air temperature, but at level about 4 °C higher than dew-point temperature, so the condensation conditions there were not existed. In the experiments the vapour moved from the rivulet into the surrounding air and the plate, but heat was transferred from surroundings and the rivulet into the plate. At these conditions the liquid microfilm see an example Fig. 1, was formed on the plate very easily. The presented research is the extension of the results described in the part I [9].

The experimental findings are presented in the dimensionless form. The dimensionless width and mass flow rate are given and derived in the paper [10]:

$$W = \frac{w}{\sqrt{\frac{\sigma}{\rho \cdot g}}}, \tag{1}$$

$$M = \frac{\dot{m}}{\sqrt{\frac{\sigma^2}{\mu \cdot g}}}. \tag{2}$$

* Tel.: +48 85 7 46 96 90; fax: +48 85 7 46 95 59.
E-mail address: gajewski@pb.edu.pl.

0017-9310/$ - see front matter © 2009 Elsevier Ltd. All rights reserved.
doi:10.1016/j.ijheatmasstransfer.2009.02.016

Nomenclature

g	gravitational acceleration
$\dot{m}$	mass flow rate
M	dimensionless mass flow rate
w	width of the rivulet
W	dimensionless rivulet width

Greek symbols

θ	contact angle
μ	dynamic viscosity
ρ	density of liquid
σ	surface tension

2.1. Observations and discussions

The presentation of the results obtained is such that these are divided into three subsections as follows: these for the increase of flow rate, these gained at decrease of the flow rate and those when the flow rate again increases. For detailed description refer to the part I [9]. Two forms of the reflected laser beam were observed on the screen: an elliptical triangle and a broken line (see in Fig. 2 in the part I [9]). The first point at which the image changed from the elliptical triangle to the broken line is labelled with the letter "B" on the graphs. Similarly, when the flow rate was decreasing, the point at which the broken line changed to the elliptically shaped triangle is denoted by the letter "E". In these experiments rivulet could expand even the elliptical triangle was observed, which did not take place in the experiments presented in the part I [9].

The experiments described here are preformed easier than those presented in the part I [9], but they both are more difficult than those with the sessile drops presented in work [11]. The investigations on the cooled surface indicate that copper, brass and aluminium behave more hydrophilic than under heating conditions. The worst hydrophilic properties were observed for copper. It exhibits more hydrophilic behaviour that those presented in the part I [9], where the copper was not only the worst wetted metal but its behaviour was like the hydrophobic material. The prediction of the best wetted metal is slightly complicated. In the most cases the lowest value of the contact angle (0° angle is for the best wetted material) shows water set on the aluminium plate with the exceptions of flows with $M \leqslant 0.00414$ in the first stage and for $M = 0.003627$ in the third one. In these cases the lowest

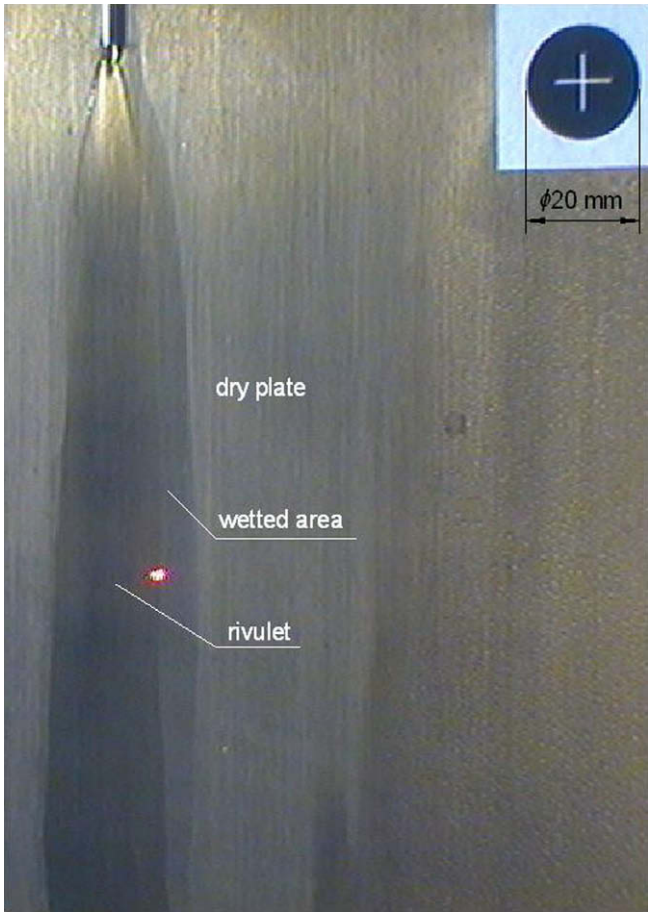

Fig. 1. The photography of rivulet on brass taken at $M = 0.00233$ (note, this picture corresponds to the first plotted point in Fig. 13). The picture shows the laser beam star and the black circle as the benchmark of a linear dimension.

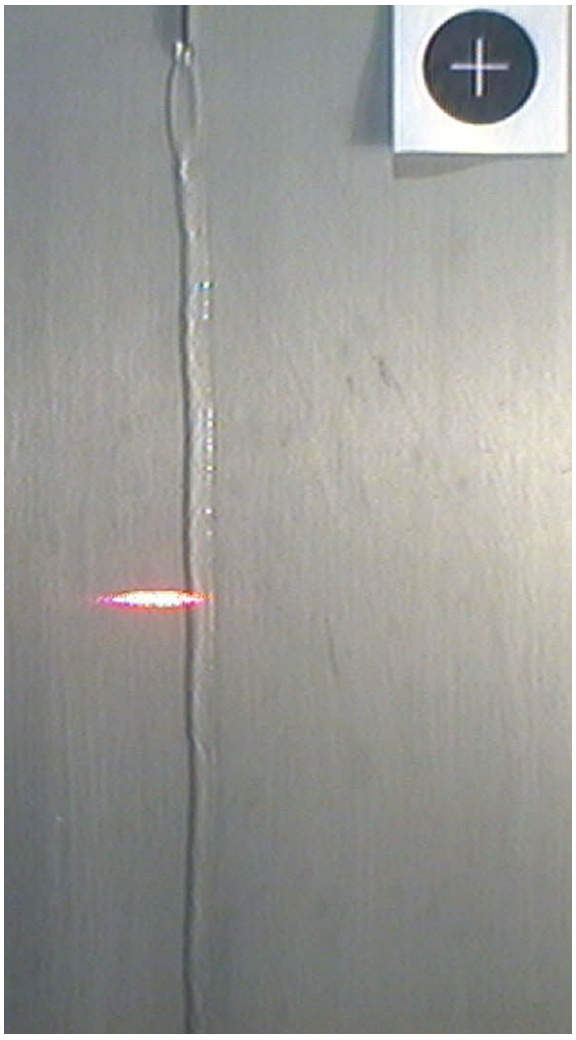

Fig. 2. The photography of rivulet on aluminium taken at $M = 0.00259$ (note, this picture corresponds to the first plotted point in Fig. 15).

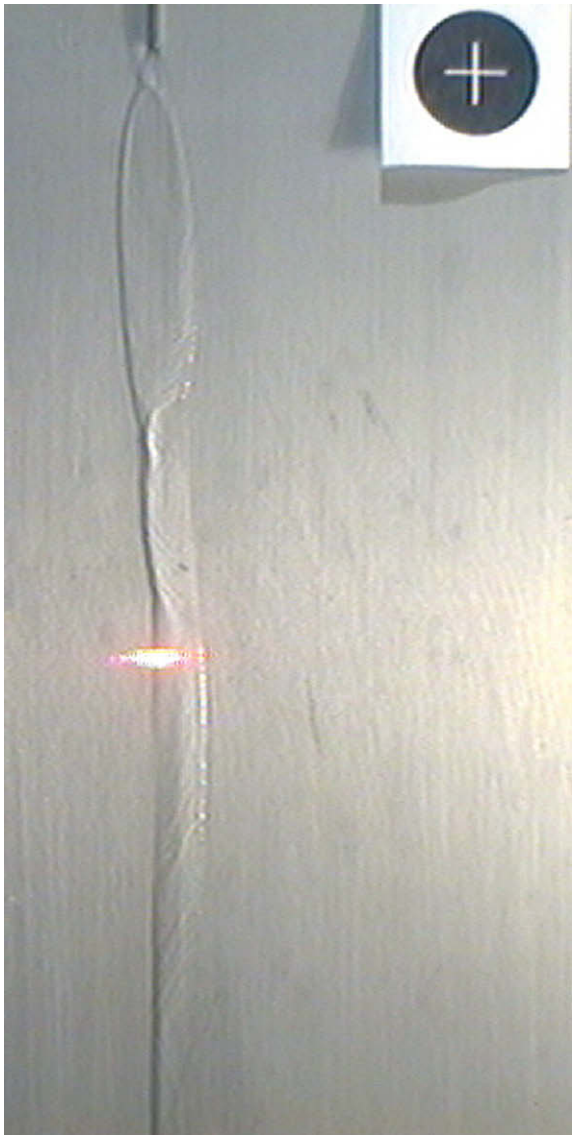

Fig. 3. The photography of rivulet on aluminium taken at $M = 0.00466$ (note, this picture corresponds to the fifth plotted point in Fig. 15).

values of the contact angle are on the brass plate. However, the area of wetted surface is more important than contact angle in the case of the mass and heat exchangers. In addition the wetting properties should be determined by the rivulet width. In that case the best wetted surface is the aluminium plate with an exception for $M < 0.006217$ in the first stage where rivulet on brass was the widest. The similar situation was presented in part I [9] where the aluminium shows the best wetted properties except the lowest flow rates in the first phase. Any movement or any curve of the rivulet across the plate was not observed as it took place in the part I [9], but the asymmetry of the rivulet was not as significant as in the previous research.

2.1.1. Wetting at increase of the flow rate

At the beginning of the experiments, it was observed that the values of the rivulet widths on the copper and aluminium plates were closed each other and even had the same value. However on the brass plate the rivulet is wider (cf. Figs. 9, 12 and 15). This situation on copper terminates when the mass flow rate is greater than $M = 0.00414$, i.e. when the rivulet flow becomes turbulent. In the case of the turbulent flow, water expands on aluminium and brass more than on copper. At the experiments presented in the part I [9] the rivulet on copper widened earlier with respect to M than on aluminium. The rivulet on brass is the widest for $M < 0.00622$, beyond this value the widest is the rivulet on aluminium. The smallest differences between the contact angle values on both sides of the rivulets are observed on the brass plate, followed by copper and aluminium. These results are much like as those described in the part I [9].

The process of the rivulet expansion on the copper plate can be divided into three stages, see in Fig. 9. The first phase is when $M \leqslant 0.00518$ and in the third one appears for $M \geqslant 0.00673$. The widening of rivulet is not great in these stages. In the second stage the rivulet widens significantly. At the beginning of the experiment (for $M \leqslant 0.00414$ under laminar or wavy flow) the mean contact angle is slightly bigger than on aluminium, at the next point taken at $M = 0.00466$ the contact angles on both materials are equal each other. At the end of this stage the contact angle increases significantly and becomes the biggest of these materials. In the second and third stages the contact angle increases and it is bigger than on brass and aluminium. For the experiments on the copper plate the big changes of the contact angle between two consecutive points were not observed. The differences in between the contact angle values on two edges are less than those presented in the part I [9].

Rivulet widening on brass develops through three stages, see in Fig. 12. At the beginning, it is the best wetted material among of the investigated: the contact angle is the lowest and the rivulet is the widest. In the first stage (for $M \leqslant 0.00373$ under laminar or wavy flow) the rivulet has a constant width and the contact angle increases. In the second phase under turbulent flow the rivulet widens, but the contact angle increases at the start and at the end points. For median flows it decreases. In the third stage (for $M \geqslant 0.00653$) the rivulet exhibits the constant width and the contact angle decreases.

The main problem observed during experiments on aluminium was the grey colour of the investigated surface, which made the dry and wetted areas very difficult to distinguish. In the case of brass, see Fig. 1, the dry plate, wetted area and rivulet are clearly distinguished. In the opposite, on the aluminium plate it is clearly seen only the dry part of the plate and area covered by water, but the wetted part and rivulet can not to be distinguished in the photography, see Fig. 4. The border between rivulet and adsorbed water is indicated in the pictures by a star made of laser beam. The process of rivulet expansion can be divided into three stages, as shown in Fig. 15. In the first one bounded by $M \leqslant 0.00414$ the rivulet slightly widens except the last point, where it is constant. In the third one spanning $M \geqslant 0.00673$ the width of the rivulet is also almost constant. In the second stage located in between $0.00414 < M < 0.00673$ the rivulet widens significantly. The contact angle decreases in the first stage except the third point for which $M = 0.00363$, where it slightly increases. At the beginning of the second stage the contact angle decreases significantly, then it increases and decreases again. The decreasing is continued at the third phase. Finally the aluminium plate is the best wetted material: the contact angle can be appreciated as the lowest and the rivulet is the widest.

The lowest differences between the contact angle values on two edges of the rivulet are on copper at the initial in flow rates and for the bigger mass flow rates under turbulent flow on each metal. In the case of copper and aluminium it takes place when $M \geqslant 0.00570$, but in the case of the brass plate it was observed at $M \geqslant 0.00466$.

The differences between the contact angle values on two edges are less than those presented in the part I [9]. Now the rivulet is much more symmetrical than that observed on the heated plate (as an example cf. Fig. 6 in part I [9] and Fig. 2 as well as Fig. 18 in part I [9] and Fig. 15).

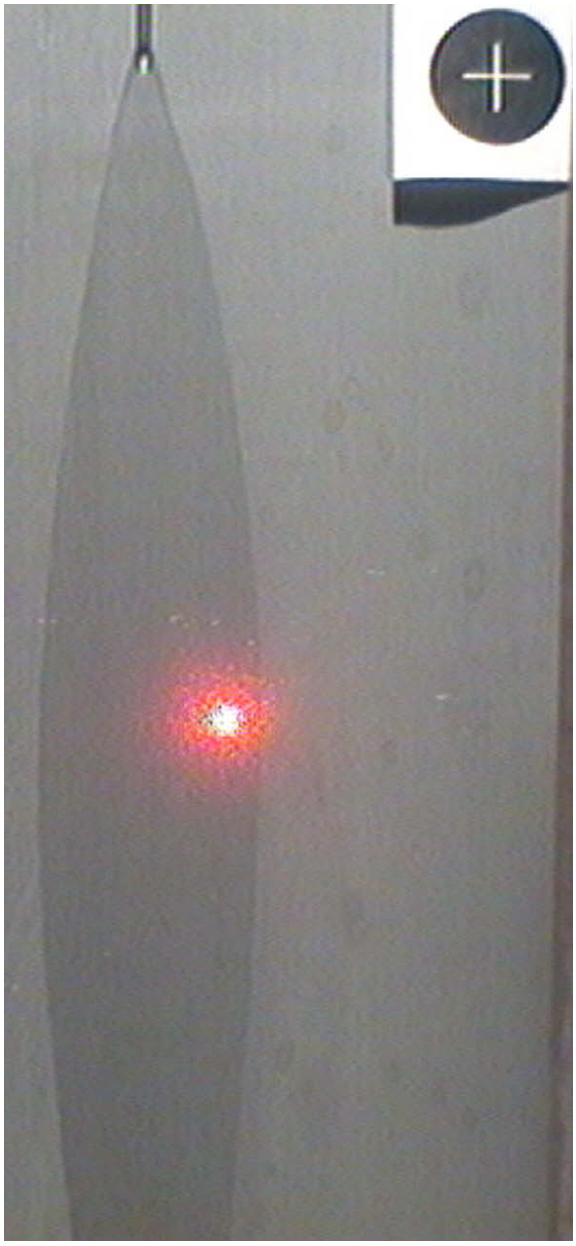

Fig. 4. The photography of rivulet on aluminium taken at $M = 0.00259$ (note, this picture corresponds to the first plotted point in Fig. 16).

2.1.2. Wetting at the decrease of the flow rate

When the flow rate decreases the discrepancies between the retreating contact angles on both edges are much smaller than those observed for the advancing angels (flow rate increases) on aluminium and brass. However these differences are only slightly smaller on copper. Regarding the rivulet width the narrowing on aluminium, brass and copper are similar and it can be classified in two stages: in the first one under turbulent flow the rivulet width is almost constant and in the second one under laminar or wavy flow the rivulet narrows significantly. Generally the contact angle decreases, the exceptions will be described below.

The width of rivulet on the copper plate remains almost constant and the contact angle becomes smaller when $0.00777 \geqslant M \geqslant 0.00414$, see in Fig. 10. In the second stage (for $M < 0.00414$) the contact angle and rivulet width are decreasing simultaneously with the exception of the last but one (second plotted) point, where the contact angle slightly increases. The rivulet is the narrowest and the contact angle is the biggest. There is an exception for the point at $M = 0.00466$, where the contact angle on brass is the biggest.

In the case of the brass plate, the width remains almost constant and the contact angle becomes smaller in the first stage (for $0.00700 \geqslant M \geqslant 0.00327$). In the second stage (for $M < 0.00327$) the contact angle and the rivulet width decrease simultaneously, see Fig. 13.

The water on aluminium does not retreat, but the contact angle falls with the exception of the second (tenth plotted) point, in the first stage (for $0.00777 \geqslant M \geqslant 0.00311$). In the second stage (for $M < 0.00311$) the width and the contact angle decrease simultaneously, see Fig. 16.

Concluding, the best hydrophilic properties are observed for aluminium, the second ones are observed for brass. The rivulet on brass is narrower than on aluminium but the rivulet width on the copper is significantly less than that on aluminium or brass.

2.1.3. Wetting the repeated increase in the flow rate

Similarly as for the increase of the flow rate on previously dry surface the rivulet widening on earlier wetted surface can be divided into three stages. However each metal exhibits different behaviour and hence must be described separately.

The rivulet on the copper plate has almost constant width at the first phase with the little increasing contact angle value, see Fig. 11. The first stage terminates at $M = 0.00415$. In the second stage under turbulent flow (for $0.00415 < M \leqslant 0.00518$) the contact angle increases rapidly, but rivulet width decreases and then increases. This situation is caused by the different process of rivulet widening, cf. Figs. 5–7. In the third stage the path of rivulet has been formed (see in Fig. 8), so that the rivulet can widen easily and the contact angle increases.

The rivulet on brass has constant width at the first stage and it is observed the laminar or wavy flow. The first four points shown on the mean contact angle graph have the same inclination to M-axis as in the case of the copper plate. In the second stage under the turbulent flow (for $0.00466 \leqslant M \leqslant 0.00560$) the rivulet widens very easily with simultaneous increase of the contact angle, see Fig. 14. In the third stage (for $M > 0.00560$) the rivulet width slightly increases and contact angle slightly decreases coupled.

The flow along the aluminium plate is laminar or wavy at the first stage then the width and contact angle increase simultaneously. The stage ends for $M = 0.003627$, see Fig. 17. In the second stage under wavy flow the width is constant and contact angle is slightly higher. In the third stage (for $M \geqslant 0.00518$) the width is the widest and contact angle increases. However, it is questionable a slightly decrease in the contact angle value in the last but one point as well as significantly less inclination of two last points on the contact angle graph than that between 6th and 9th points. This different situation may be caused by the measurements error. Moreover, in the second stage somewhat similar situation is observed: the rivulet does not widen and contact angle value increases only slightly. In these cases it is supposed that rivulet could have increased its thickness in the inner part of the stream (between edges) and the edges might have not affected by any change.

The best wetted material is aluminium. It has the widest rivulet with the smallest values of the contact angle, except two points: for $M = 0.00327$ and $M = 0.00373$, where the slightly lower contact angle values are on the brass plate, cf. Figs. 14 and 17. The next very good wetted material is brass. The worst wetted properties are observed on copper, the rivulet is the most narrow and the contact angles are the highest except one point: at $M = 0.00466$, where the contact angle on brass has the biggest value cf. Figs. 11, 14 and 17.

Fig. 5. The photography of rivulet on copper taken at $M = 0.004145$ (note, this picture corresponds to the fourth plotted point in Fig. 11).

Fig. 6. The photography of rivulet on copper taken at $M = 0.004663$ (note, this picture corresponds to the fifth plotted point in Fig. 11).

2.1.4. Comparison of the results

Decrease of temperature improves the wetting properties of the investigated materials. The water rivulet becomes wider, in the case of the flow along aluminium or brass even much wider than on the plates with heated surface. In conclusion the material is better wetted. However, some exceptions in the case of the contact angle values are observed.

On the brass plate, when the mass flow rate was decreased, the tree points with the lowest mass flow rate values shown in Fig. 16 presented in the part I [9] have almost the same values as the corresponding points in Fig. 13. The same situation is observed when the mass flow rate is increased repeatedly for the second time: the first four points have almost the same values, cf. Fig. 17 given in the part I [9] and Fig. 14.

When the mass flow rate was decreased, cf. Fig. 19 in the part I [9] and Fig. 16 the analogous behaviour has been observed on the aluminium plate for the tree points with the lowest mass flow rate values. Another difference is observed in the range $0.00674 > M > 0.00363$, where contact angle values on the heated plate are lower than those on the cooled one. When the flow rate is increased for the second time the contact angle values are close on heated and cooled plates at the start point and the bigger values are observed in the both experiments in turns up to $M = 0.00622$, cf. Fig. 20 in the part I [9] and Fig. 17. For higher mass flow rate values the contact angle on heated plate is much higher than on cooled one.

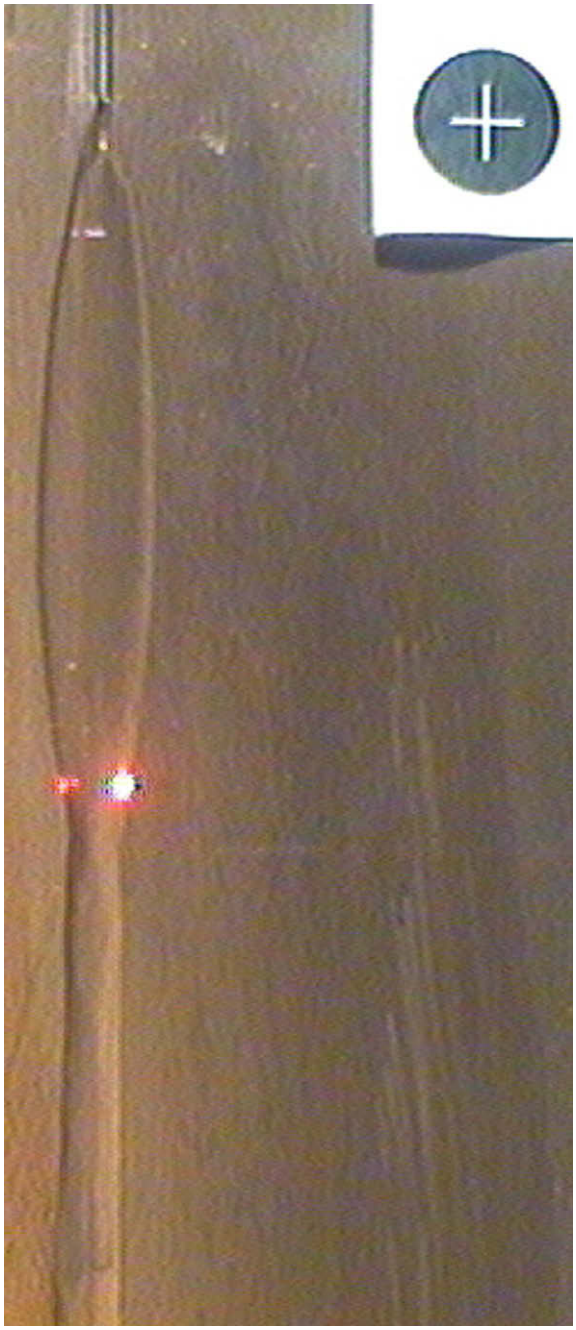

Fig. 7. The photography of rivulet on copper taken at $M = 0.005181$ (note, this picture corresponds to the sixth plotted point in Fig. 11).

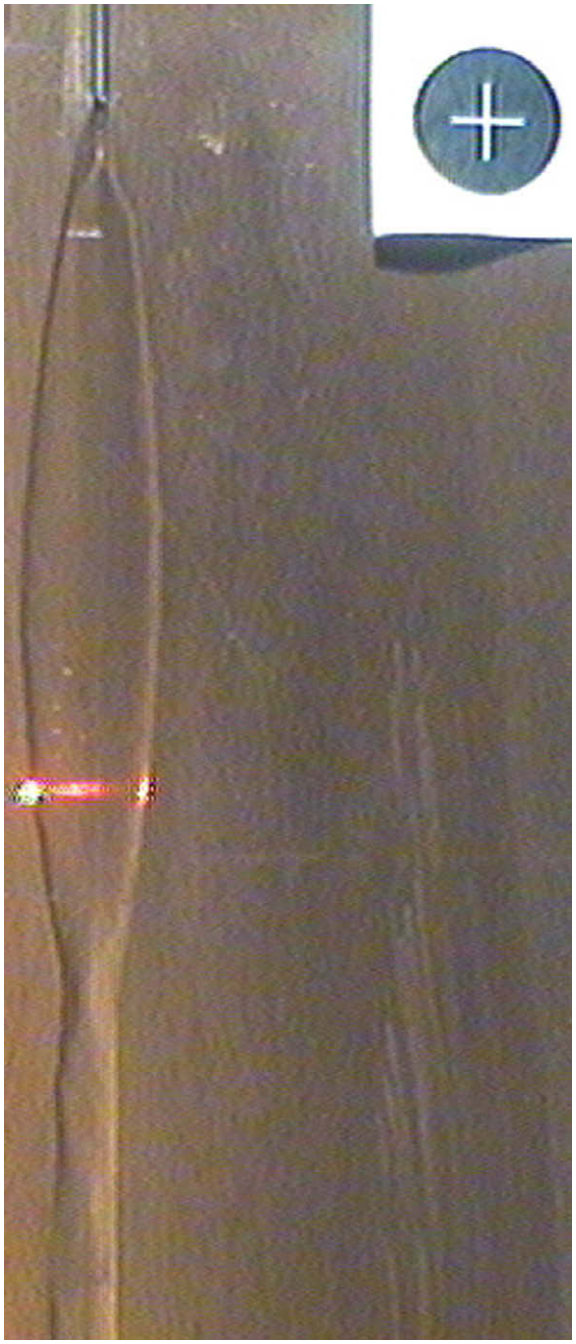

Fig. 8. The photography of rivulet on copper taken at $M = 0.005699$ (note, this picture corresponds to the seventh plotted point in Fig. 11).

This behaviour can be explained as follows: cooling of the plate favours the existence of the liquid film on the solid phase surface. As a consequence, the oxide barriers on aluminium and zinc under cooling conditions are removed completely at the lower mass flow rate values than under heating conditions. It is also observed widening of the rivulet before the broken line was noted, cf. Fig. 15. It did not appear on the heated plate.

The presented experiments confirm discrepancy between wetting properties of water under static and dynamic conditions described in the part I [9].

There has been also observed considerably unexpected situations on the aluminium and brass plates: while the mass flow rate was increasing the width was constant or slightly increased, but the contact angle decreased. These situations can be observed on the graphs: two last points in Fig. 12, three last points in Fig. 14, two first and three last points in Fig. 15, the fourth and fifth points as well as the ninth and tenth points in Fig. 17. In Fig. 16, it has been observed the opposite trends: while the mass flow rate was decreasing the width did not change, but the contact angle increased, see two points with the biggest mass flow rate shown in Fig. 16. Each observation described above could be explained as due to measurement errors. However six independent observations coupled can lead to a conclusion that the rivulet might change only in the inner part of the stream and the edges might have not affected by any change.

A segment of the circle is assumed at works [5–7,10] as the shape of the rivulets to model their flow. This assumption can be

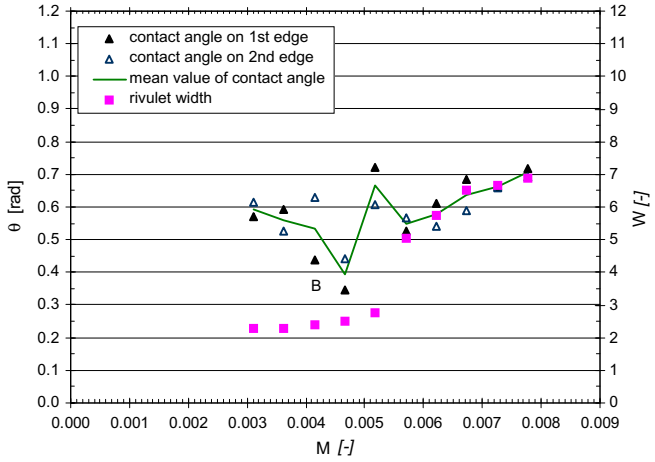

Fig. 9. Advancing contact angle on both edges and width of the rivulet on a copper plate with a roughness (Ra) of 0.38 μm.

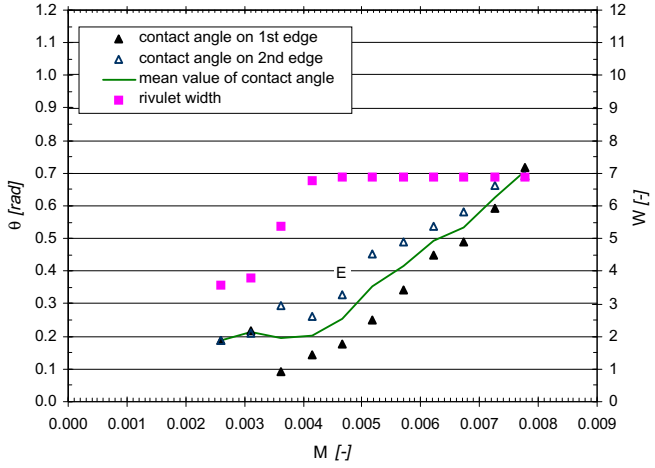

Fig. 10. Retreating contact angle on both edges and width of the rivulet on a copper plate with a roughness (Ra) of 0.38 μm.

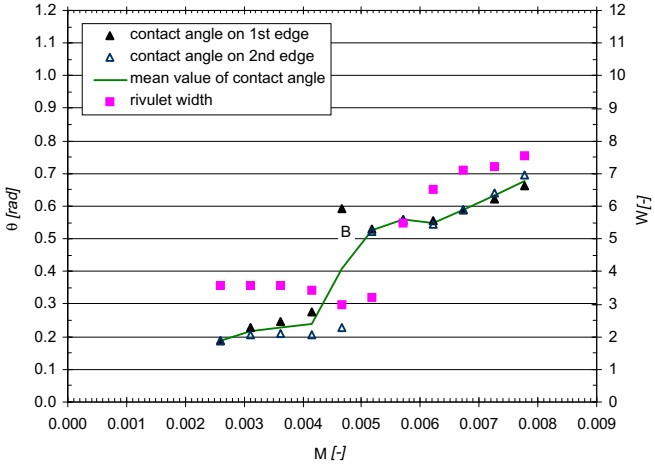

Fig. 11. Advancing contact angle on both edges and width of the rivulet on a copper plate with a roughness (Ra) of 0.38 μm, when the flow rate was increased again.

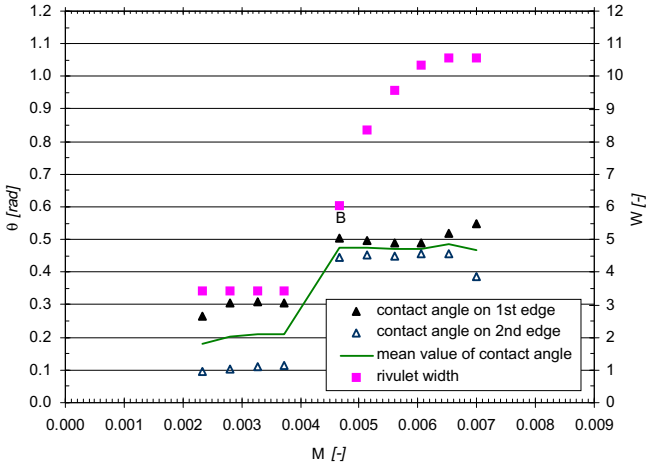

Fig. 12. Advancing contact angle on both edges and width of the rivulet on a brass plate with a roughness (Ra) of 1.6 μm.

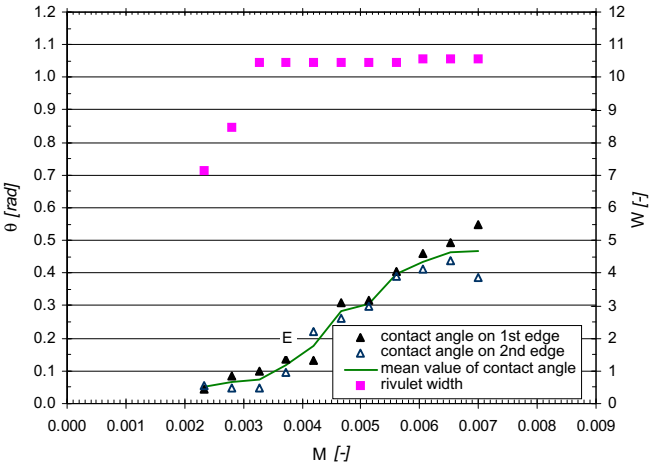

Fig. 13. Retreating contact angle on both edges and width of the rivulet on a brass plate with a roughness (Ra) of 1.6 μm.

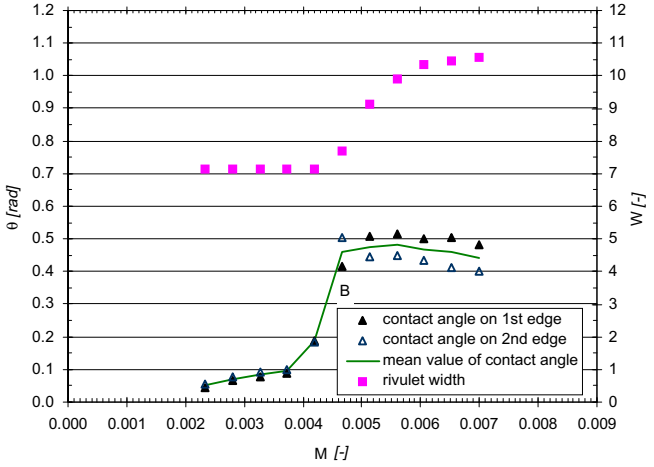

Fig. 14. Advancing contact angle on both edges and width of the rivulet on a brass plate with a roughness (Ra) of 1.6 μm, when the flow rate was increased again.

made only for less laminar flows. If there are exist significant differences between contact angle values on two edges or there is observed an asymmetry of the rivulet (e.g. see in Fig. 3), the segment of the circle is not allowed to be assumed for analysis.

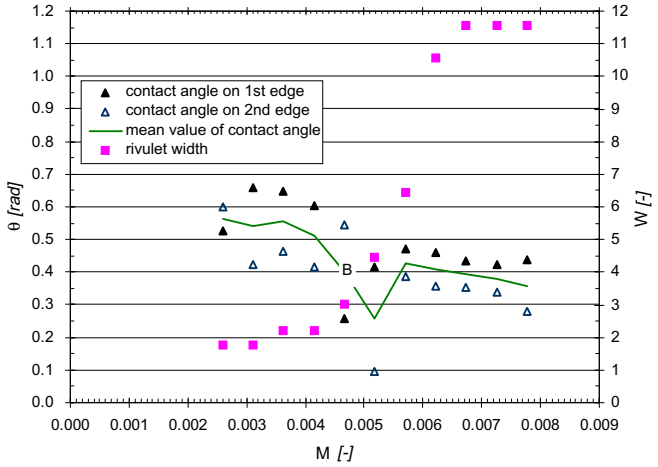

Fig. 15. Advancing contact angle on both edges and width of the rivulet on an aluminium plate with a roughness (Ra) of 1.38 μm.

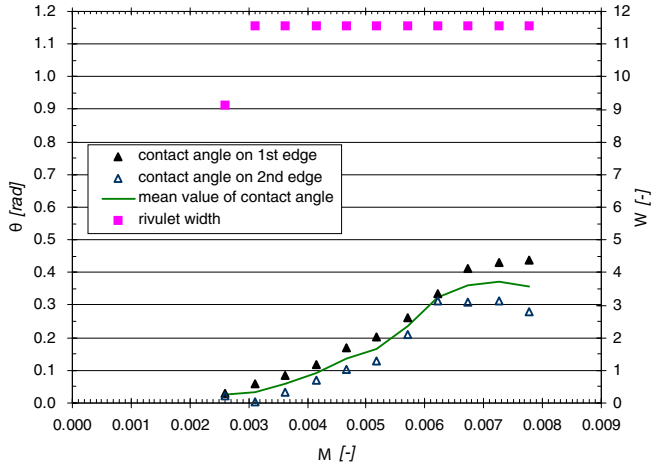

Fig. 16. Retreating contact angle on both edges and width of the rivulet on an aluminium plate with a roughness (Ra) of 1.38 μm.

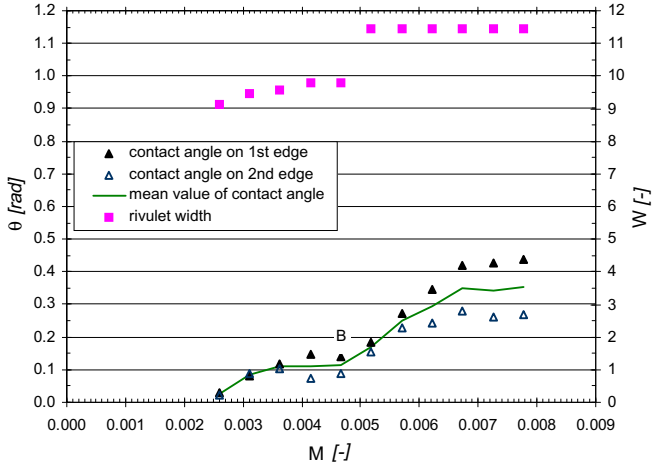

Fig. 17. Advancing contact angle on both edges and width of the rivulet on an aluminium plate with a roughness (Ra) of 1.38 μm, when the flow rate was increased again.

3. Conclusions

Comparisons among experiments under flow conditions with heated and cooled surfaces as well as under static conditions confirm conclusions presented in the part I [9]:

1. The wetting properties examined for sessile drops cannot be extrapolated to rivulets.
2. The wetting properties of dipole liquids on a metal surface are different under flow (dynamic) conditions and static conditions.
3. The contact angle should be measured on both edges of the rivulet.
4. The more electrons there are on the last metal shell, the more hydrophilic properties a metal has under flow conditions.

Additionally it is observed that:

5. Lower surface temperature improves the wetability of the metals,
6. Lower temperature causes the oxide barriers on aluminium or zinc surface to remove at the lower mass flow rate.
7. It will be no impact of temperature on the contact angle values under laminar flow if the brass plate is previously wetted.
8. There will be no influence of temperature on the contact angle values in some particular situations, if the aluminium plate is previously wetted.

Since there are different contact angles on two opposite rivulet edges, it concludes that

9. It is not allowed to assume a segment of a circle as the rivulet shape.

Acknowledgement

The scientific work was funded by a grant from The State Committee for Scientific Research between 2003 and 2006.

References

[1] I. Langmuir, V.J. Schaefer, The effect of dissolved salts on insoluble monolayers, I. J. Am. Chem. Soc. 59 (1937) 2405.
[2] G.D. Towell, L.B. Rothfeld, Hydrodynamics of rivulet flow, AIChE J. 12 (5) (1966) 972–980.
[3] S. Semiczek-Szulc, J. Mikielewicz, Experimental investigations of contact angles of rivulets flowing down a vertical solid surface, Int. J. Heat Mass Transfer 21 (1978) 1625.
[4] S. Hirasawa, E.G. Hauptmann, Dynamic contact angle of a rivulet flowing down a vertical heated wall, 8th International Heat Transfer Conference, San Francisco, CA, USA 4 (1986) 17–22.
[5] J. Mikielewicz, J.R. Moszynski, Minimum thickness of liquid film flowing vertically down a solid surface, Int. J. Heat Mass Transfer 19 (1976) 771–776.
[6] J. Mikielewicz, J.R. Moszynski, An improved analysis of breakdown of thin liquid films, Arch. Mech. 30 (4-5) (1978) 489–500.
[7] Y. Sutjiadi-Sia, R. Eggers, Lateral wetting angle of falling film in dense fluid, Int. J. Heat Mass Transfer 51 (2008) 3608–3614.
[8] A. Gajewski, A method for contact angle measurements under flow conditions, Int. J. Heat Mass Transfer 48 (2005) 4829–4834.
[9] A. Gajewski, Contact Angle, Rivulet width hysteresis on metallic surfaces. Part I: with heated surface, Int. J. Heat Mass Transfer 51 (2008) 5762–5771.
[10] A. Gajewski, M. Trela, Effect of rivulet mass flow rate on the surface wetted area, Arch. Thermodyn. 23 (1-2) (2002) 101–125.
[11] A. Gajewski, Contact angle and sessile drop diameter hysteresis on metal surfaces, Int. J. Heat Mass Transfer 51 (2008) 4628–4636.